forests

MDPI

Article

Evaluation of O_3 Effects on Cumulative Photosynthetic CO_2 Uptake in Seedlings of Four Japanese Deciduous Broad-Leaved Forest Tree Species Based on Stomatal O_3 Uptake

Masahiro Yamaguchi [1,2], Yoshiyuki Kinose [3,4], Hideyuki Matsumura [5] and Takeshi Izuta [6,*]

1 Graduate School of Agriculture, Tokyo University of Agriculture and Technology, Fuchu, Tokyo 183-8509, Japan
2 Graduate School of Fisheries and Environmental Sciences, Nagasaki University, Nagasaki 852-8521, Japan
3 United Graduate School of Agricultural Science, Tokyo University of Agriculture and Technology, Fuchu, Tokyo 183-8509, Japan
4 Graduate Faculty of Interdisciplinary Research, University of Yamanashi, Kofu, Yamanashi 400-8510, Japan
5 Environmental Science Research Laboratory, Central Research Institute of Electric Power Industry, Abiko, Chiba 270-1194, Japan
6 Institute of Agriculture, Tokyo University of Agriculture and Technology, Fuchu, Tokyo 183-8509, Japan
* Correspondence: izuta@cc.tuat.ac.jp; Tel.: +81-42-367-5728

Received: 9 May 2019; Accepted: 29 June 2019; Published: 2 July 2019

Abstract: The current level of tropospheric ozone (O_3) is expected to reduce the net primary production of forest trees. Here, we evaluated the negative effects of O_3 on the photosynthetic CO_2 uptake of Japanese forest trees species based on their cumulative stomatal O_3 uptake, defined as the phytotoxic O_3 dose (POD). Seedlings of four representative Japanese deciduous broad-leaved forest tree species (*Fagus crenata*, *Quercus serrata*, *Quercus mongolica* var. *crispula* and *Betula platyphylla* var. *japonica*) were exposed to different O_3 concentrations in open-top chambers for two growing seasons. The photosynthesis–light response curves (*A*-light curves) and stomatal conductance were measured to estimate the leaf-level cumulative photosynthetic CO_2 uptake (ΣP_{n_est}) and POD, respectively. The whole-plant-level ΣP_{n_est} were highly correlated with the whole-plant dry mass increments over the two growing seasons. Because whole-plant growth is largely determined by the amount of leaf area per plant and net photosynthetic rate per leaf area, this result suggests that leaf-level ΣP_{n_est}, which was estimated from the monthly *A*-light curves and hourly PPFD, could reflect the cumulative photosynthetic CO_2 uptake of the seedlings per unit leaf area. Although the O_3-induced reductions in the leaf-level ΣP_{n_est} were well explained by POD in all four tree species, species-specific responses of leaf-level ΣP_{n_est} to POD were observed. In addition, the flux threshold appropriate for the linear regression of the responses of relative leaf-level ΣP_{n_est} to POD was also species-specific. Therefore, species-specific responses of cumulative photosynthetic CO_2 uptake to POD could be used to accurately evaluate O_3 impact on the net primary production of deciduous broad-leaved trees.

Keywords: Japanese deciduous broad-leaved trees; net photosynthetic rate; net primary production; stomatal O_3 uptake; phytotoxic O_3 dose

1. Introduction

Tropospheric ozone (O_3) has detrimental effects on vegetation [1–3]. Current O_3 levels adversely affect growth and physiological functions, such as the photosynthesis of forest tree species [4,5]. Because of this phytotoxicity, net primary production (NPP) and biomass accumulation by temperate

forests were estimated to be reduced by 1–16% [6]. Therefore, O_3 indirectly affects radiative forcing through its adverse effects on photosynthetic CO_2 uptake [7]. Despite robust evidence for the negative impact of O_3 on plant productivity, the indirect effect of O_3 on radiative forcing was not mentioned in the Intergovernmental Panel on Climate Change Fifth Assessment report because of a lack of corroborating studies [8]. In Asia, an increase in the surface O_3 concentration is expected, although the changes in its concentration depend on the emission scenario [9–11]. In Japan, despite a decrease in the concentrations of O_3 precursors, the surface O_3 concentration has been increasing because of a reduction in NO titration and an increase in transboundary air pollution [12]. Therefore, it is necessary to quantify the negative impact of O_3 on the photosynthetic CO_2 uptake of Japanese forest tree species to account for the indirect effect of O_3 on radiative forcing.

Ozone enters leaves through their stomata and damages their cellular components [13–15]. Because the real impacts of O_3 on plants mainly depend on the amounts of O_3 reaching the sites of damage within the leaves, these impacts can be quantified by measuring the cumulative stomatal O_3 uptake, defined as phytotoxic O_3 dose (POD) and associated response functions [16–18]. Because the degree of stomatal opening adjusts continuously to environmental changes [19], this O_3 flux-based approach requires the development of mathematical models to estimate the POD in leaves, using stomatal responses to environmental factors [20–22]. In Japan, several researchers have established multiplicative models to estimate the POD in the leaves of forest tree species [23–27]. In addition to modeling stomatal O_3 uptake, the degree of the O_3-induced reduction in photosynthetic CO_2 uptake should be evaluated, based on the POD, to quantify the negative impact of O_3 on the NPP.

According to a meta-analysis by Wittig et al. (2007) [28], the light-saturated net photosynthetic rate (A_{sat}) decreases at a rate of 0.22% per mmol O_3 m^{-2} leaf area (LA) as POD increases. Because the relationship between POD and the percent change in A_{sat} varies with species and genotypes within species, as well as with locations and experimental conditions, little of the variability in the degree of percent change in A_{sat} is accounted for by the POD [28]. In addition to this variability, seasonal variation in the degree of O_3-induced reduction in A_{sat} could explain why POD is responsible for only a small percentage of the changes in A_{sat} measured at a certain time. For example, the degree of O_3-induced reduction in A_{sat} of *Populus nigra* is lower in autumn than in summer [29], whereas POD is greater in autumn than in summer owing to the longer accumulation period. Because POD could be related to cumulative O_3 damage, a cumulative O_3 effects on net photosynthesis is an appropriate dependent variable in the response function of photosynthetic CO_2 uptake to POD. Therefore, it is necessary to evaluate the degree of O_3 damage on the cumulative photosynthetic CO_2 uptake at leaf-level, which could be easily incorporated into models of the carbon cycling, throughout an entire growing season, taking into consideration of seasonal and diurnal changes in the O_3 damage on A_{sat}.

In Japan, temperate deciduous forests have been classified into three forest types: cool temperate deciduous forests, warm temperate deciduous forests and cool temperate mixed deciduous broadleaf/conifer forests [30]. The dominant tree species are *Fagus crenata*, *Quercus serrata* and *Quercus mongolica* var. *crispula*, respectively [30] and *Betula platyphylla* var. *japonica* is a typical early successional species in these forest types [31]. There are considerable differences in the sensitivities of these tree species to O_3 concentration, as evaluated by whole-plant growth [32,33]. Although a stomatal conductance model to estimate the PODs in the leaves of these tree species has been established [27], the degree of O_3 damage on cumulative photosynthetic CO_2 uptake has not been evaluated based on the POD. Therefore, in the present study, we conducted an experimental study on the effects of O_3 on cumulative photosynthetic CO_2 uptake in the leaves of four representative Japanese deciduous broad-leaved tree species with different O_3 sensitivities. To account for seasonal and diurnal changes in the degree of the O_3-induced reduction in net photosynthetic rate when estimating the cumulative O_3 effects on photosynthetic CO_2 uptake, we measured photosynthesis–light response curves (*A*-light curves) monthly throughout an entire growing season.

2. Materials and Methods

2.1. Plant Materials and Growth Conditions

In December 2011, 3-year-old seedlings of *F. crenata* and 2-year-old seedlings of *Q. serrata*, *Q. mongolica* var. *crispula* and *B. platyphylla* var. *japonica* were individually planted in 1/2000 Wagner's pots (volume: 12 L, diameter: 240 mm, depth: 258.5 mm) filled with commercial horticultural soil (Takii & Co., Ltd., Kyoto, Japan). The N, P and K contents in the potted soil were 320, 210 and 300 mg L^{-1}, respectively. On 25 April 2012, the seedlings were transferred into 12 rectangular open-top chambers (OTCs, 13.0 m^2 of growth space and 2.4 m in height) located at the Akagi Testing Center of the Central Research Institute of Electric Power Industry (Maebashi, Gunma, Japan) and eight seedlings per species were grown in each chamber. To measure the initial whole-plant dry mass (WDM), including belowground parts, the 10 seedlings of each species, which were not assigned to the chamber and whose mean height and stem base diameter were similar with those of the seedlings assigned to the chambers, were harvested, dried at 80°C in an oven for more than 5 days and weighed. The initial WDMs of *F. crenata*, *Q. serrata*, *Q. mongolica* var. *crispula* and *B. platyphylla* var. *japonica* seedlings were 11.1 ± 5.2 g, 36.9 ± 8.1 g, 23.7 ± 5.51 g and 11.1 ± 1.8 g, respectively (±SD, n = 10). The latitude, longitude and elevation above sea level at the experimental site are 36°28′ N, 139°11′ E and 540 m, respectively. In late August 2012 and in late April and late July 2013, the seedlings were rotated among and inside the OTCs to minimize variation among the OTCs for each treatment and among the seedlings within the OTC owing to chamber and positional effects, respectively. All the seedlings were regularly irrigated to keep the potted soil moist. On 12 April and 5 July 2013, all the seedlings were fertilized with 8 g m^{-2} of a slow-release solid fertilizer (N:P:K = 8:8:8, Ohmiya Green Service Co., Ltd., Saitama, Japan) to avoid the nutrient deficiency, which could limit physiological processes. The air temperature, relative air humidity and photosynthetic photon flux density (PPFD) inside the OTCs were monitored during the experimental period from 26 April 2012 to 14 November 2013 (Table S1). The vapor pressure deficit (VPD) was calculated from the saturated vapor pressure, which was calculated from air temperature and the relative air humidity.

2.2. Gas Treatment

From 26 April to 22 November 2012 and from 29 March to 14 November 2013, the seedlings were exposed to charcoal-filtered (CF) air or O_3 at 1.0, 1.5 or 2.0 times the ambient concentration in the OTCs. For each treatment, three chamber replications, for a total of 12 chambers, were used. The ambient O_3 concentration was independently monitored by a UV absorption O_3 analyzer (ML9810, Teledyne Monitor Labs, Englewood, CO, USA) at the experimental site. Ozone was generated from oxygen-enriched dry air by an electrical discharge O_3 generator (Oz-24-UA, Ebara Corporation, Japan) and injected into the OTCs through a water trap that removed the nitrogen byproducts produced by the O_3 generator [34]. The O_3 concentrations at 90 cm above the OTC floors were monitored using the UV absorption O_3 analyzer. The O_3 concentration accumulated over a threshold of 40 nmol mol^{-1} (ppb) (AOT40) is used to investigate the concentration-based critical levels for O_3 impact on vegetation. Thus, whether the O_3 concentration in the present study was above the level having negative impact on vegetation, could be investigated, even though the AOT40 is biologically less relevant than POD in O_3 impact assessments on vegetation [18]. Consequently, we calculated AOT40 as the sum of the differences between the hourly mean O_3 concentrations and 40 ppb when the former exceeded 40 ppb during the daylight hours and the solar irradiation was greater than 50 W m^{-2}.

2.3. Measurement of Stomatal Diffusive Conductance

The stomatal diffusive conductance to water vapor (g_{sw}, mmol H_2O m^{-2} LA s^{-1}) in the leaves of the seedlings was measured using an LI-1600 steady-state porometer (LI-COR, Lincoln, NE, USA). Throughout the O_3-exposure period, the measurements were conducted on the abaxial sides of the 1st flush leaves of *F. crenata*, the 1st and 2nd flush leaves of *Q. serrata* and *Q. mongolica* var. *crispula* and the

early and late leaves of *B. platyphylla* var. *japonica* seedlings. Corresponding PPFD, air temperature, relative air humidity, soil volumetric water content (SWC, %) at a 10-cm depth from the surface of the potted soil and O_3 concentration were also recorded. The measurements were conducted throughout the daytime on the representative leaves at a rate of about two days per month during the growing seasons.

2.4. Calculation of POD

The POD with a flux threshold of Y nmol O_3 m^{-2} LA s^{-1} (POD_Y, mmol O_3 m^{-2} LA), during one growing season, was calculated according to the method described by CLRTAP (2017) and Kinose et al. (2014) [18,27], with modifications of the parameters in the stomatal conductance model based on the g_{sw} obtained in the present study. The period used to calculate the POD_Y was from the day of leaf emergence of each leaf type to the day on which the net photosynthetic rate was measured for each growing season. The POD_Y during the daylight hours was calculated by accumulating stomatal O_3 flux (F_{st}, nmol O_3 m^{-2} LA s^{-1}) with or without a flux threshold of Y nmol O_3 m^{-2} LA s^{-1} (POD_Y or POD_0, respectively). The F_{st} was calculated using the following equation:

$$F_{st} = \frac{[O_3]_{air} - [O_3]_{leaf}}{r_{b\_ozone} + r_{s\_ozone}} \quad (1)$$

where $[O_3]_{air}$ and $[O_3]_{leaf}$ represent O_3 concentrations in the air and the intercellular space (nmol O_3 mol^{-1}), respectively, and r_{b_ozone} and r_{s_ozone} represent boundary layer resistance and stomatal resistance for O_3 diffusion, respectively. For each gas treatment, the average hourly mean O_3 concentration of three chambers was used for $[O_3]_{air}$. The $[O_3]_{leaf}$ was assumed to be zero [35]. The r_{b_ozone} was calculated from the crosswind leaf dimension (L_d, m) and wind speed (u, m s^{-1}) as follows:

$$r_{b\_ozone} = 1.3 \times 150 \times \sqrt{\frac{L_d}{u}} \quad (2)$$

where the factor 1.3 accounts for the difference in diffusivity between heat and O_3 [18]. Average L_d values for *F. crenata*, *Q. serrata*, *Q. mongolica* var. *crispula* and the early and late leaves of *B. platyphylla* var. *japonica* seedlings were 0.014, 0.015, 0.023, 0.012 and 0.032 m, respectively. The average wind speed 1.5 m above the OTC floors was 0.17 m s^{-1}. The r_{s_ozone}, the reciprocal of the hourly mean stomatal diffusive conductance to O_3 (g_{sO3}, mmol O_3 m^{-2} s^{-1}), was calculated from the hourly mean g_{sw} and a conversion factor of 0.663 was used to account for the difference in the molecular diffusivity of O_3 and that of water vapor in air [18,36]. The hourly mean g_{sw} was estimated using the stomatal conductance model reported by Kinose et al. (2014) [27]:

$$g_{sto} = g_{max} \times f_{phen} \times f_{light} \times \max\left[f_{min}, \left(f_{temp} \times f_{VPD} \times f_{SWC} \times f_{O3conc}\right)\right] \quad (3)$$

where g_{sto} represents the estimated hourly mean g_{sw} and g_{max} represents the species-specific maximum g_{sw}. The parameters f_{phen}, f_{light}, f_{min}, f_{temp}, f_{VPD}, f_{SWC} and f_{O3conc} were all expressed in relative terms (i.e., values between 0 and 1) as a proportion of g_{max}, where f_{phen} represents the modification of g_{max} owing to leaf phenological changes; f_{light} represents the modification of g_{max} by PPFD (μmol m^{-2} s^{-1}); f_{min} represents the relative value of species-specific minimum g_{sw} with respect to g_{max}; f_{temp} represents the modification of g_{max} by air temperature (T, °C); f_{VPD} represents the modification of g_{max} by VPD (kPa); f_{SWC} represents the modification of g_{max} owing to SWC (%); and f_{O3conc} represents the reduction in g_{max} resulting from the acute effect of O_3 (ppb). We used the boundary line analysis to define the parameters of each f in the relationships between the ratio of g_{sw} to g_{max} and environmental factors [37]. For details of each f and how to analyze the relationships using the boundary line analysis, please refer to Kinose et al. (2014) [27]. Results of the parameterization of stomatal conductance models for the leaves of *F. crenata*, *Q. serrata*, *Q. mongolica* var. *crispula* and *B. platyphylla* var. *japonica* seedlings

are shown in Table S3. The POD_0 in the leaves of the tree species during both growing seasons are presented in Tables S2 and S4.

2.5. Measurement of A-Light Curves

From May to November 2012 and from April to October 2013, the *A*-light curves of the seedlings were measured monthly using an infrared gas analyzer system (LI-6400, LI-COR Inc, Lincoln, Nebraska, US). Two to four seedlings from each chamber were randomly selected to be measured. The seedlings were moved from the OTCs into an experimental room and the measurements were made using three LI-6400s in the room to avoid the influences of weather conditions at the measurement time. The measurements were conducted on one leaf from each leaf type per seedling for the 1st flush leaves of *F. crenata*, the 1st and 2nd flush leaves of *Q. serrata* and *Q. mongolica* var. *crispula* and the early and late leaves of *B. platyphylla* var. *japonica* seedlings. Because the leaf emergence of *B. platyphylla* var. *japonica* is heterophyllous [31] and the late leaves emerge successively, the measurements were conducted for the 4th and 5th, 9th and 10th, 15th and 16th (only in 2013) and 18–20th late leaves, as counted from the base of the 1st or 2nd branch from the top of the seedlings. The last measurement day of each growing season was the time when the leaves were almost yellowed at the end of the growing season. When we did not find target leaf for the measurement of *A*-light curve due to leaf abscission by the exposure to O_3, we did not measure it. The *A*-light curves were determined at an atmospheric CO_2 concentration of 390 μmol CO_2 mol^{-1} and a relative air humidity of approximately 60% inside the leaf chamber. As much as possible, the target air temperature inside the leaf chamber was the 10-year average of the monthly mean of the daily maximum air temperature inside the OTCs used in the present study. The actual air temperatures inside the leaf chamber differed among the month and ranged from 17.5 °C to 26.0 °C in 2012 and from 19.0 °C to 28.9 °C in 2013. For detailed information, please refer to the Table S5. To obtain the response of net photosynthetic rate to PPFD, after acclimation of the leaves to light-saturated conditions at a PPFD of 1500 ± 1 μmol m^{-2} s^{-1}, PPFD was gradually reduced to zero and the net photosynthetic rates were recorded under PPFDs of 1500, 1,000, 500, 250, 100, 50 and 0 μmol m^{-2} s^{-1}. To obtain the *A*-light curve, a non-rectangular hyperbolic function was fitted to the response of the net photosynthetic rate to PPFD. Although photosynthetic parameters other than the *A*-light curve could offer a better indication of the overall damage of O_3 on photosynthesis and its mechanisms, we did not measure the parameters, because we focused on the effects of O_3 on the cumulative photosynthetic CO_2 uptake rather than the mechanisms underlying the O_3-induced reduction in net photosynthesis.

2.6. Calculation of Cumulative Photosynthetic CO_2 Uptake

The cumulative photosynthetic CO_2 uptake per unit LA (mol CO_2 m^{-2} LA s^{-1}) during each growing season was calculated as the sum of the product of time (1 h) and estimated hourly value of net photosynthetic rate (P_{n_est}, μmol CO_2 m^{-2} LA s^{-1}) over one growing season (ΣP_{n_est}, mol CO_2 m^{-2} LA). The P_{n_est} was calculated from the hourly mean PPFD monitored inside the OTCs and the *A*-light curves that were obtained monthly. The PPFD was the mean value of the 12 OTCs. The *A*-light curves were the means of the three chamber replicates for each treatment. When the hourly mean of PPFD was 0 μmol m^{-2} s^{-1}, P_{n_est} was not calculated and was not summed up for the ΣP_{n_est}. The calculation period was from the first to the last measurement days of the *A*-light curve for each growing season. In each growing season, the *A*-light curve obtained from the first measurement was used to calculate P_{n_est} during the period from the first measurement day to the middle day of the subsequent measurement day. The *A*-light curve obtained from the last measurement was used to calculate P_{n_est} during the period from the middle day of the previous measurement day to the last measurement day. The *A*-light curves, other than those obtained from the first and last measurements in each growing season, were used to calculate P_{n_est} from the middle day of the previous measurement day to the middle day of the subsequent measurement day (approximately 1 month). This calculation assumed the step-changes in the *A*-light curve between the two measurement days. Because the ΣP_{n_est}

is time integral of P_{n_est}, ΣP_{n_est} calculated by assuming linear changes in A-light curve between the two measurement days would result in the same value. When there was no target leaf owing to O_3-induced early leaf abscission (e.g., Tables S6 and S7), we did not accumulate the P_{n_est} for ΣP_{n_est}. The monthly A-light curves of each species are shown in Table S6.

The sums of the product of the number of day and the A_{sat} at PPFD of 1500 μmol m^{-2} s^{-1} (μmol CO_2 m^{-2} LA s^{-1}) over one growing season (ΣA_{sat} × days, μmol CO_2 m^{-2} LA s^{-1} day) were calculated for each treatment and each growing season as a possible indicator of O_3-induced percent changes in ΣP_{n_est}. The A_{sat}, which was recorded when the A-light curve was measured and the number of days during the growing season were used to calculate ΣA_{sat} × days. The periods for the ΣA_{sat} × days was the same as those for the ΣP_{n_est}. The A_{sat} measured on the first measurement day was multiplied by the number of days during the period from the first measurement day to the middle of the subsequent measurement day. The A_{sat} that was measured on the last measurement day was multiplied by the number of days during the period from the last measurement day to the middle of the previous measurement day. The A_{sat}, other than those measured on the first and last measurement days, were multiplied by the number of days from the middle day of the previous measurement to that of the subsequent measurement (approximately 1 month). The products of the A_{sat} and the number of days were summed for ΣA_{sat} × days during each growing season. The monthly A_{sat} are shown in Table S7. The ΣP_{n_est} and ΣA_{sat} × days in the leaves of *F. crenata*, *Q. serrata*, *Q. mongolica* var. *crispula* and *B. platyphylla* var. *japonica* seedlings are indicated in Table S4.

2.7. Validation of Cumulative Photosynthetic CO_2 Uptake

To validate the calculation of leaf-level ΣP_{n_est}, leaf-level ΣP_{n_est} was expanded from a LA basis to a whole-plant basis and we analyzed the relationship of the whole-plant-level ΣP_{n_est} with WDM increments over the two growing seasons. The numbers of each leaf type per plant were counted periodically during the growing seasons. Part of each leaf type was sampled to measure the area per leaf using an area meter (LI-3100, Li-Cor Inc, Lincoln, Nebraska, USA). Leaf area per plant of each leaf type was estimated from the product of leaf number per plant and mean area per leaf. For the calculation of the whole-plant-based ΣP_{n_est}, the product of P_{n_est} and estimated leaf area per plant was summed up during each growing season. To measure the WDM at the end of the gas exposure, the seedlings of each tree species were harvested in October and November 2013. The harvested seedlings were dried at 80 °C in an oven for more than 5 days and weighed. The WDM increments over the two growing seasons were calculated using the initial and final WDMs. The effects of O_3 on the WDMs of *F. crenata*, *Q. serrata*, *Q. mongolica* var. *crispula* and *B. platyphylla* var. *japonica* seedlings in October and November 2013 are shown in Table S8.

2.8. Relationships of POD with ΣP_{n_est} and A_{sat}

For each tree species, the ΣP_{n_est} or A_{sat} in the CF treatment was used as a reference (100%) to calculate the relative value of ΣP_{n_est} or A_{sat} (%), respectively, in each gas treatment. It has been suggested that the form of the Weibull function ($Y = a \times \exp[-(X/\omega)^{\lambda}]$) is a biologically realistic response curve through the discussion on the function as a part of the National Crop Loss Assessment Network (NCLAN) in the USA [38]; therefore, this function was fitted to the response of relative ΣP_{n_est} or A_{sat} to POD without a flux threshold (POD_0). According to the method of CLRTAP (2017) [18], in addition, the response functions of relative ΣP_{n_est} to POD with different flux thresholds (POD_Y) were analyzed using a linear regression analysis to determine any species-specific responses of ΣP_{n_est} to POD. In these analyses, the data obtained from different leaf types (i.e., 1st and 2nd flush leaves or early and late leaves) were pooled for each species, because the responses of the different leaf types were similar. The period for the POD calculation was from the leaf emergence day to each measurement day of A-light curves for A_{sat} or to the last measurement day of the A-light curves for ΣP_{n_est}.

3. Results

Table 1 shows the air temperature, VPD and PPFD inside the chambers during the O_3-exposure periods from 26 April to 22 November 2012 and from 29 March to 14 November 2013. The climatic conditions inside the OTCs were similar during the exposure periods of 2012 and 2013.

Table 1. Seasonal means of air temperature, vapor pressure deficit (VPD), and photosynthetic photon flux density (PPFD) inside open-top chambers (OTCs) during the O_3-exposure period in 2012 and 2013.

Period	Air Temperature (°C)						VPD (kPa)				PPFD	
	Daily Mean		Daily Max.[a]		Daily Min.[b]		Daily Mean		Daily Max.[a]		(mol m^{-2} day^{-1})	
26 Apr.–22 Nov., 2012	19.4	(0.1)	25.0	(0.3)	15.2	(0.0)	0.41	(0.03)	1.28	(0.06)	16.9	(0.2)
29 Mar.–14 Nov., 2013	19.1	(0.1)	25.2	(0.3)	14.6	(0.1)	0.43	(0.04)	1.32	(0.09)	16.8	(0.3)

Each value is the mean value of 12 OTCs; the standard deviation is shown in parentheses. [a] Mean daily 1-h maximum value. [b] Mean daily 1-h minimum value.

Table 2 shows the average O_3 concentrations and AOT40 of O_3 in each gas treatment during the O_3-exposure periods of 2012 and 2013. The exclusion efficiency of O_3 in the CF treatment was about 80%. Averaged across the two growing seasons, even though the seasonal mean O_3 concentrations in the 1.5× and 2.0×O_3 treatments were 1.62–1.74 and 2.19–2.33 times higher than that in the 1.0×O_3 treatment, respectively, the highest 1-h maximum O_3 concentration in the two treatments almost reached the target concentration (i.e., 1.53 and 2.02 times, respectively). The average concentration in 2012 was lower than that in 2013, whereas the daily 1-h maximum concentration was higher in 2012 than in 2013. Although this result suggests a stronger diel pattern in 2012, it was not obvious. The daylight AOT40 in the 1.0 × O_3 treatments in 2012 and 2013 were 6.0 and 7.5 ppm h and exceeded the concentration-based critical level for O_3-sensitive forest trees (5 ppm h) that was adopted by the United Nations Economic Commission for Europe Convention on Long-Range Trans-boundary Air Pollution [18].

Table 2. O_3 concentrations and AOT40 of O_3 during the O_3-exposure period in 2012 and 2013.

Period	Treatment	Concentration (nl l^{-1})								Daylight	
		Seasonal Mean						Highest		AOT40 [b]	
		24-h Mean		12-h Mean[a]		1-h Max.		1-h Max.		(µl l^{-1} h)	
26 Apr.–22 Nov., 2012 (211 days)	CF	4.4	(0.4)	4.6	(0.4)	7.4	(0.6)	21.5	(1.5)	0.0	(0.0)
	1.0 × O_3	25.2	(0.3)	28.1	(0.4)	41.0	(0.7)	111.5	(7.5)	6.0	(0.2)
	1.5 × O_3	43.9	(0.7)	46.5	(0.6)	71.2	(0.6)	165.0	(4.0)	33.7	(0.1)
	2.0 × O_3	59.1	(0.8)	64.5	(0.7)	93.3	(0.3)	216.0	(2.0)	70.4	(1.5)
29 Mar.–14 Nov., 2013 (231 days)	CF	4.9	(0.2)	5.2	(0.3)	8.8	(0.6)	25.5	(0.5)	0.0	(0.0)
	1.0 × O_3	26.9	(0.3)	31.2	(0.4)	43.2	(0.9)	90.3	(3.6)	7.5	(0.6)
	1.5 × O_3	47.1	(0.3)	49.5	(0.5)	69.4	(0.9)	143.3	(0.6)	34.9	(1.3)
	2.0 × O_3	62.2	(0.3)	65.4	(0.2)	92.5	(1.1)	190.3	(2.5)	69.6	(0.9)

Each value is the mean of three chamber replicates, and the standard deviation is shown in parentheses. CF: charcoal-filtered air; 1.0 × O_3: 1.0 times the ambient O_3 concentration; 1.5 × O_3: 1.5 times the ambient O_3 concentration; 2.0 × O_3: 2.0 times the ambient O_3 concentration. [a] 12 h: 6:00–18:00. [b] Daylight AOT40: Accumulated exposure over a threshold of 40 nl l^{-1} during daylight hours (global radiation > 50 W m^{-2}).

To test the performance of stomatal conductance model for the leaves of *F. crenata*, *Q. serrata*, *Q. mongolica* var. *crispula* and *B. platyphylla* var. *japonica* seedlings, linear regression analyses were conducted between measured g_{sw} and g_{sw} estimated from the model of Kinose et al. (2014) [27], with modifications of g_{max} and the parameters of each function (Table 3). The model parameterized in the present study accounted for 48.2% of the variation in the 1st flush leaves of *F. crenata*, 41.6% and 34.7% of the variation in the 1st and 2nd flush leaves of *Q. serrata*, respectively, 34.6% and 20.9% of

the variation in the 1st and 2nd flush leaves of *Q. mongolica* var. *crispula*, respectively and 30.6% and 30.1% of the variation in the early and late leaves of *B. platyphylla* var. *japonica*, respectively. We did not evaluate the performance of stomatal conductance model using the g_{sw} and corresponding meteorological parameters obtained from the sites different from the present experiment site.

Table 3. Results of the linear regression analyses of the measured stomatal diffusive conductance to water vapor (g_{sw}, mmol H_2O m^{-2} LA s^{-1}) and g_{sw} estimated from the model of Kinose et al. (2014), using the modifications of g_{max} and the parameters of each function based on the g_{sw} obtained in the present study.

	F. crenata	*Q. serrata*		*Q. mongolica* var. *crispula*		*B. platyphylla* var. *japonica*	
	1st Flush (n = 351)	**1st Flush (n = 312)**	**2nd Flush (n = 191)**	**1st Flush (n = 374)**	**2nd Flush (n = 166)**	**Early (n = 352)**	**Late (n = 662)**
Slope	0.854	0.871	0.752	0.843	0.659	0.691	0.697
Intercept	29.0	40.5	88.4	72.4	135.2	113.7	253.1
R^2 value	0.482	0.416	0.347	0.346	0.209	0.306	0.301
RMSE [a]	66.9	69.9	113.7	113.5	170.8	116.8	296.2
MBE [b]	7.1	29.8	61.5	30.3	60.5	71.8	185.1

[a] RMSE: Root mean square error of the stomatal conductance model (mmol H_2O m^{-2} LA s^{-1}); [b] MBE: Mean bias error of the stomatal conductance model (mmol H_2O m^{-2} LA s^{-1}).

The relationships between WDM increments and the whole-plant-based ΣP_{n_est} during the two growing seasons are shown in Figure 1. The values are plotted for each species across all the treatments. There were significant positive correlations for *F. crenata* and *Q. mongolica* var. *crispula* but those for *Q. serrata* and *B. platyphylla* var. *japonica* were not significant.

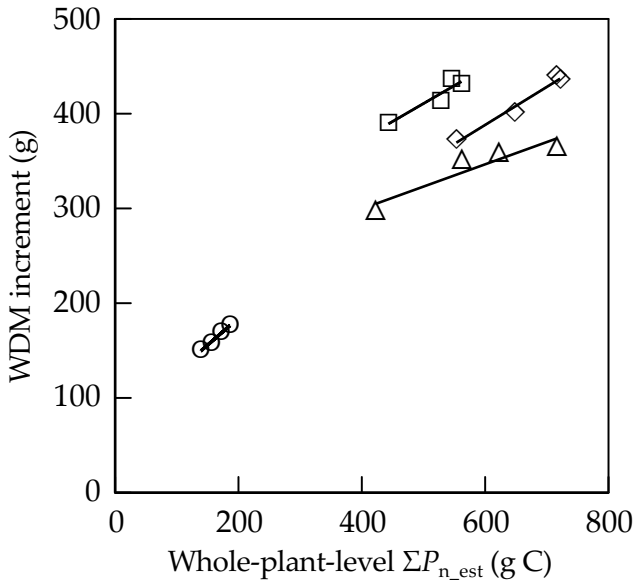

Figure 1. Relationships between the whole-plant-level ΣP_{n_est} and whole-plant dry mass (WDM) increment over the two growing seasons. Solid lines indicate the regression line for each species. ○: *F. crenata* ($y = 0.569x + 70.5$, $R^2 = 0.984$, $p < 0.01$), □: *Q. serrata* ($y = 0.378x + 222$, $R^2 = 0.890$, not significant), ◇: *Q. mongolica* var. *crispula* ($y = 0.401x + 147$, $R^2 = 0.975$, $p < 0.05$), △: *B. platyphylla* var. *japonica* ($y = 0.235x + 205$, $R^2 = 0.868$, not significant).

The responses of relative A_{sat} or relative ΣP_{n_est} to POD_0 in the leaves of *F. crenata*, *Q. serrata*, *Q. mongolica* var. *crispula* and *B. platyphylla* var. *japonica* are shown in Figure 2a–h. The coefficients of determination (R^2) for the response functions of relative A_{sat} or relative value of leaf-level ΣP_{n_est} to POD_0 were 0.663 and 0.894 in *F. crenata*, respectively, 0.645 and 0.935 in *Q. serrata*, respectively,

0.591 and 0.833 in *Q. mongolica* var. *crispula*, respectively and 0.602 and 0.760 in *B. platyphylla* var. *japonica*, respectively.

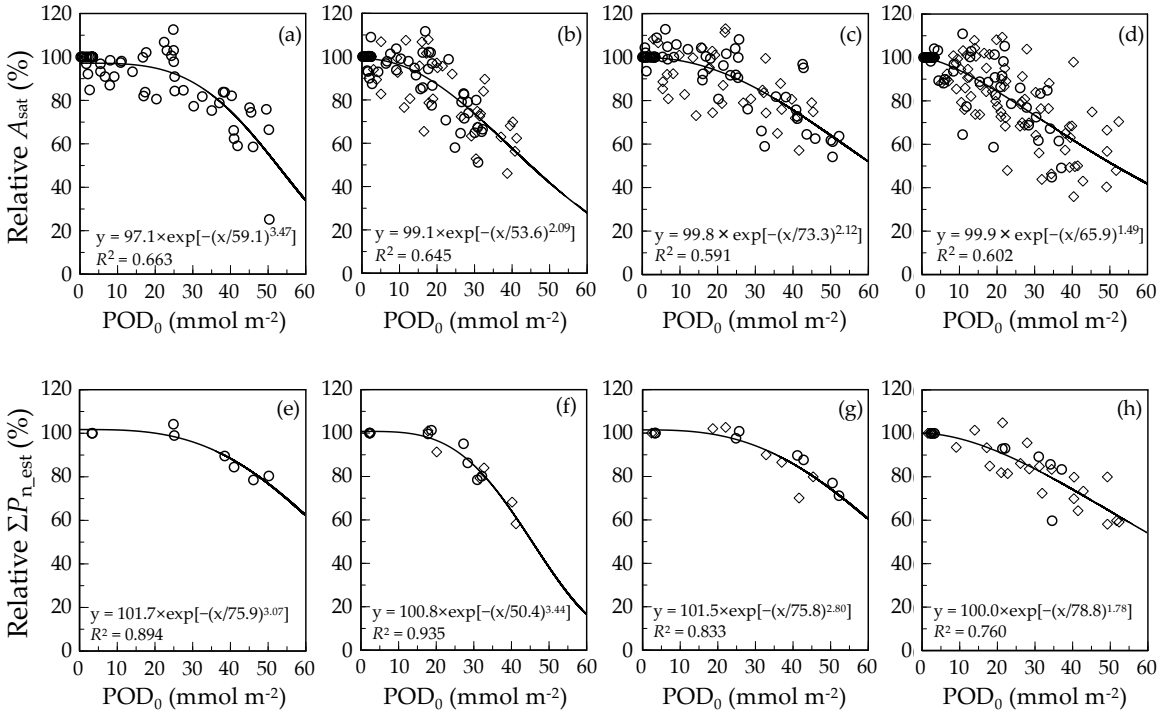

Figure 2. Relationships between relative A_{sat} (**a**–**d**) or ΣP_{n_est} (e–h) and POD without flux threshold (POD_0) in the leaves of *F. crenata* (**a**,**e**), *Q. serrata* (**b**,**f**), *Q. mongolica* var. *crispula* (**c**,**g**) and *B. platyphylla* var. *japonica* (**d**,**h**). Open circles indicate 1st flush or early leaves, and open diamonds indicate 2nd flush or late leaves. The Weibull function was fitted to the response, and the coefficient of determination (R^2) is indicated in each figure. Data in (**a**)–(**d**) were from Table S2 (POD_0) and S7 (A_{sat}), and in (**e**)–(**h**) were from Table S4 (POD_0 and ΣP_{n_est}).

To discuss the species-specific responses of ΣP_{n_est} to POD, we examined the flux threshold appropriate for the linear regression of the responses of ΣP_{n_est} to POD_Y (Table 4). The POD_Y appropriate for the linear regression of the response were POD_7 for *F. crenata*, POD_4 for *Q. serrata*, POD_8 for *Q. mongolica* var. *crispula* and POD_3 for *B. platyphylla* var. *japonica*.

Table 4. The R^2 value for the linear regression line between relative value of leaf-level ΣP_{n_est} and phytotoxic O_3 dose (POD_Y, Y: flux threshold) in the leaves of *F. crenata*, *Q. serrata*, *Q. mongolica* var. *crispula* and *B. platyphylla* var. *japonica* seedlings.

Tree Species	No. of Plot	Y										
		0	**1**	**2**	**3**	**4**	**5**	**6**	**7**	**8**	**9**	**10**
F. crenata	*n* = 8	0.710 **	0.747 **	0.805 **	0.850 **	0.881 ***	0.903 ***	0.917 ***	0.921 ***	0.918 ***	0.903 ***	0.878 ***
Q. serrata	*n* = 16	0.724 ***	0.776 ***	0.839 ***	0.879 ***	0.893 ***	0.884 ***	0.858 ***	0.817 ***	0.764 ***	0.704 ***	0.653 ***
Q. mongolica var. *crispula*	*n* = 16	0.697 ***	0.730 ***	0.780 ***	0.824 ***	0.861 ***	0.889 ***	0.909 ***	0.921 ***	0.925 ***	0.918 ***	0.900 ***
B. platyphylla var. *japonica*	*n* = 36	0.738 ***	0.754 ***	0.768 ***	0.775 ***	0.774 ***	0.767 ***	0.755 ***	0.740 ***	0.722 ***	0.703 ***	0.681 ***

Statistical significance for R^2 is shown: ** $p < 0.01$ and *** $p < 0.001$.

In Figure 3, the relationships between the relative value of ΣP_{n_est} and that of $\Sigma A_{sat} \times$ days in the leaves of *F. crenata*, *Q. serrata*, *Q. mongolica* var. *crispula* and *B. platyphylla* var. *japonica* are shown. There was a significant positive linear correlation between the relative value of ΣP_{n_est} and that of $\Sigma A_{sat} \times$ days.

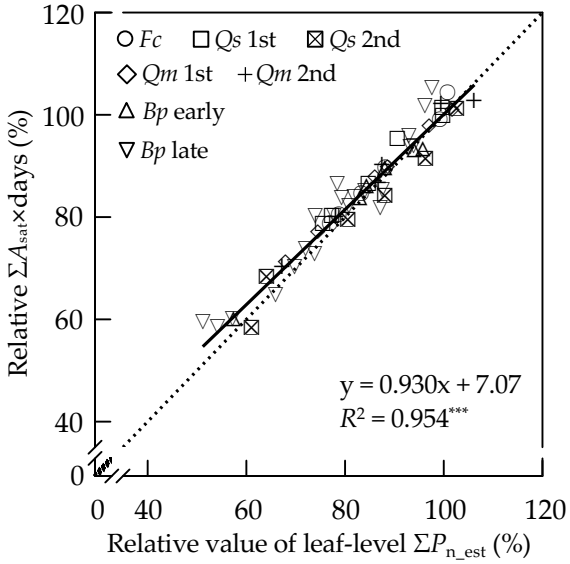

Figure 3. Relationship between the relative value of leaf-level ΣP_{n_est} (%) and relative $\Sigma A_{sat} \times$ days (%) in the 1st flush leaves of *F. crenata* (*Fc*), the 1st and 2nd flush leaves of *Q. serrata* (*Qs* 1st and *Qs* 2nd, respectively), the 1st and 2nd flush leaves of *Q. mongolica* var. *crispula* (*Qm* 1st and *Qm* 2nd, respectively), and the early and late leaves of *B. platyphylla* var. *japonica* (*Bp* early and *Bp* late, respectively). Datasets for the charcoal-filtered air (CF) treatment were not plotted. The relationship was analyzed by linear regression. Solid and dashed lines indicate the regression line and 1:1 line, respectively. The equation and the coefficient of determination (R^2) of the regression line are indicated in the figure. Significance for the R^2 is shown: *** $p < 0.001$.

4. Discussion

In the present study, we evaluated the negative effects of O_3 on leaf-level photosynthetic CO_2 uptake, which could be easily incorporated into models of the carbon cycling, in the seedlings of four representative Japanese deciduous broad-leaved forest tree species based on POD. Lombardozzi et al. (2013) [39] compiled and analyzed the response of A_{sat} to POD using data from the peer-reviewed literature. Although the overall decrease in A_{sat} was observed, high variance masked any correlations between the decline in A_{sat} with increase in POD. Because POD could be related to cumulative O_3 damages, it could correspond not to O_3 effect on net photosynthetic rate at a certain time but to that on cumulative photosynthetic CO_2 uptake. Several researchers observed that the extent of the O_3-induced reduction in net photosynthetic rate varied seasonally [29,40]. On the other hand, Coleman et al. (1995) [41] observed a greater extent of O_3-induced reduction in net photosynthetic rate under high light intensities compared with under low light intensities, indicating variations in the extent of the O_3 damage on photosynthetic CO_2 uptake during the daytime and among canopy positions owing to diurnal variation in the light intensity and self-shading, respectively. In the present study, to take such seasonal and diurnal variations into account, we estimated ΣP_{n_est} from *A*-light curves measured monthly and diurnal changes in PPFD throughout the entire growing season. Because this estimation assumes that the *A*-light curves have been constant for about one month and ignored the diurnal changes in air temperature and relative air humidity, it was necessary to validate the estimation. For this purpose, we expanded the ΣP_{n_est} from a LA basis to the whole-plant basis by considering a roughly estimated LA per plant and whole-plant-level ΣP_{n_est} was compared with WDM increment over two growing seasons. Although not all the species showed significant correlations between WDM

increment and the whole-plant-level ΣP_{n_est} during the two growing seasons (Figure 1), all the species had relatively high R^2 values. In general, whole-plant growth is largely determined by the amount of leaf area per plant and net photosynthetic rate per leaf area. Although the LA per plant was roughly estimated and calculation of ΣP_{n_est} did not consider the effects of environmental condition other than light intensity on photosynthetic CO_2 uptake, these results suggest that the leaf-level ΣP_{n_est} could reflect the cumulative photosynthetic CO_2 uptake of the seedlings per unit LA, which could be easily incorporated into models of the carbon cycling.

Because the negative impact of O_3 on photosynthetic CO_2 uptake can indirectly increase radiative forcing [7], we evaluated the effect of O_3 on photosynthetic CO_2 uptake based on POD_0 in the leaves of representative Japanese deciduous broad-leaved tree species. According to the meta-analysis by Wittig et al. (2007) [28], the 28% of variation in the O_3-induced percent changes in A_{sat} measured at a certain time was accounted for by the linear function of POD_0 (i.e., R^2 value was 0.28). On the other hand, Lombardozzi et al. (2013) [39] did not observe any correlations between changes in A_{sat} and POD owing to the large variability across studies. In the present study, about 60% of O_3-induced percent changes in the A_{sat} was accounted for by POD_0 (Figure 2a–d), which is greater than Wittig et al. (2007) [28]. However, the POD_0 accounted for the O_3-induced percent changes in the ΣP_{n_est} rather than those in the A_{sat} (Figure 2e–h). These results suggest that the ΣP_{n_est} is an appropriate dependent variable in the response function of photosynthetic CO_2 uptake to POD, which could result from the fact that the cumulative stomatal O_3 uptake corresponds to the extent of cumulative O_3 effect on photosynthetic CO_2 uptake. Therefore, the response function of relative leaf-level ΣP_{n_est} to POD is useful for the quantification of the negative impact of O_3 on the NPP of forests.

In the present analysis, there are uncertainties in the calculations of leaf-level ΣP_{n_est}, whole-plant-level ΣP_{n_est} and POD. For the calculation of leaf-level ΣP_{n_est}, the calculation period was from the first day of the first measurement of *A*-light curve to the last day of the last measurement in each growing season. Because this period was shorter than actual accumulation period, the leaf-level ΣP_{n_est} could underestimate the actual cumulative photosynthetic CO_2 uptake per unit LA. It is unclear that the ignorance of the effects of changes in air temperature and air humidity on the *A*-light curves causes overestimation or underestimation, but it would be the source of the error. Furthermore, it is also unclear the measurement of *A*-light curve at about one-month interval was enough time resolution to estimate the leaf-level cumulative photosynthetic CO_2 uptake. The greater the number of measurements during the growing season, the better for the estimation of absolute value of accumulated photosynthetic CO_2 uptake. In the present study, however, we focused on the extent of O_3-induced reduction in leaf-level ΣP_{n_est}, rather than absolute value. Because there were relatively high R^2 value in the relationship between WDM increment and the whole-plant-level ΣP_{n_est} in all tree species, the monthly measurement of *A*-light curve could be enough time resolution for the evaluation of O_3 effects on cumulative photosynthetic CO_2 uptake. For the scaling up ΣP_{n_est} from leaf-level to whole-plant-level, it is necessary to account for the difference in the light condition within the canopy and the changes in the leaf area per plant not only owing to the leaf emergence but also owing to the O_3-induced leaf abscission. The calculation of whole-plant-level ΣP_{n_est} did not consider the shelf-shading within the canopy and assumed that all leaves received full sunlight, which could result in the overestimation of the cumulative photosynthetic CO_2 uptake at whole-plant level. The estimation of changes in the leaf area per plant of tree species having flush-type leaf emergence, such as *F. crenata*, *Q. serrata* and *Q. mongolica* var. *crispula*, could be relatively easy. However, changes in the leaf area of *B. platyphylla* var. *japonica* having heterophyllous leaf emergence type is not easy to estimate, because it is difficult to identify the emergence day of each leaf, which could result in the higher variability than the other three tree species. The source of error in the calculation of POD could be estimation of g_{sw} in addition to the difficulty in the definition of leaf emergence day (i.e., start day of accumulation period) especially in *B. platyphylla* var. *japonica*. In the present study, the accuracy of estimation of g_{sw} was relatively low, especially for 2nd flush leaves of *Q. mongolica* var. *crispula* and early and late leaves of *B. platyphylla* var. *japonica*. On the other hand, mean bias error (MBE) in

the relationship between estimated and measured g_{sw} were higher than 0 in all tree species (Table 3), indicating the overestimation of g_{sw} and thus resulting in overestimation of POD. Although we did not try adjusting other parameters to get a better fit, higher accuracy in the estimation of g_{sw} is foundational to calculating the POD. Further study is required to improve the accuracy of the estimation of g_{sw} by modification of the stomatal conductance model, considering the other parameters such as O_3-induced stomatal sluggishness (e.g., Hoshika et al., 2014 [42]).

Sitch et al. (2007) [7] quantitatively evaluated the O_3-induced reduction in global gross primary production (GPP) using the sensitivity to O_3 of the whole-plant growth of European beech, birch and oak and Norway spruce for forest trees. In their report, there was considerable difference in the O_3-induced reduction in GPP between the estimations considering a low or high plant O_3 sensitivity. Thus, an uncertainty in the estimation of the O_3-induced reduction in GPP could result from different sensitivities to O_3 among tree species. There are many forest tree species with species-specific O_3 sensitivity in Asia [32,33,43]. In the present study, the species-specific responses (i.e., O_3 sensitivities) of cumulative photosynthetic CO_2 uptake to stomatal O_3 uptake were clearly demonstrated (Figure 2e–h). In addition, the flux threshold appropriate for the linear regression of the responses of relative ΣP_{n_est} to POD_Y was also species-specific (Table 4). Therefore, the differences in the O_3-sensitivity among the representative temperate forest tree species should be taken into account for more accurate and quantitative evaluations of O_3 effects on photosynthetic CO_2 uptake.

According to a meta-analysis by Wittig et al. (2007) [28], the O_3 sensitivity of A_{sat} in the leaves of trees as assessed by the POD was 0.21% per mmol O_3 m^{-2} LA. To compare the POD-based O_3 sensitivities, we conducted a linear regression analysis of the relationship between POD_0 and relative A_{sat}. The slopes of the regression lines for each tree species were −0.69, −0.95, −0.66 and −0.98% per mmol O_3 m^{-2} LA for *F. crenata*, *Q. serrata*, *Q. mongolica* var. *crispula* and *B. platyphylla* var. *japonica*, respectively. These results indicate that the POD-based O_3 sensitivity of the A_{sat} of Japanese deciduous broad-leaved forest tree species is high compared with those of the tree species reported by Wittig et al. (2007) [28], although the POD-based O_3 sensitivity reported by Wittig et al. (2007) [28] varied greatly owing to differences in species, genotypes, locations and experimental conditions. Because it has been suggested that the degree of O_3 damage is determined by the balance between stomatal O_3 flux and leaf cellular detoxification [14,44,45], the higher POD-based O_3 sensitivity of the net photosynthesis in the leaves of Japanese deciduous broad-leaved tree species could be attributed to the lower detoxification capacity of O_3 in the leaves.

Among the four tree species used in the present study, there were obvious differences in the POD-based O_3 sensitivities of cumulative photosynthetic CO_2 uptake (Figure 2e–h). At a lower POD_0 up to around 20–30 mmol O_3 m^{-2}, ΣP_{n_est} of *F. crenata*, *Q. serrata* and *Q. mongolica* var. *crispula* were less responsive to increasing POD_0 as compared with that of *B. platyphylla* var. *japonica* which showed an almost constant reduction as POD_0 increased (Figure 2e–h). The extent of the pronounced plateau at a lower POD_0 suggests a tolerance to the O_3 taken into the leaves and is represented by the variable λ in the Weibull function [37], which were 3.07, 3.44, 2.80 and 1.78 in *F. crenata*, *Q. serrata*, *Q. mongolica* var. *crispula* and *B. platyphylla* var. *japonica*, respectively (Figure 2e–h). Matyssek et al. (2007) [46] supposed that leaf mass per area (LMA) reflects the depth of the biochemical defenses against O_3 taken into the leaves, and thus it could be used as an indicator of the leaf cellular detoxification capacity of O_3. In the present study, we measured LMA at the end of each growing season (data not shown). Although there was considerable variation in the LMA between the years and among the treatments within one species, there was a significant positive correlation between the λ and median LMA of each species ($R = 0.970$, $n = 4$, $p < 0.05$). This result suggests that, among the four tree species, different responses at a lower POD_0 might result from differences in detoxification capacity in the leaves.

Among the three tree species showing λ of around 3, the response of relative ΣP_{n_est} to increasing POD_0 of *Q. serrata* become drastically sensitive above the POD_0 of around 30 mmol O_3 m^{-2}. Because the activity of antioxidative enzymes and antioxidant concentration increases in response to O_3 exposure [15,47,48], the different responses of ΣP_{n_est} to increasing POD_0 above the POD_0 of around

30 mmol O_3 m^{-2} might be caused by the difference in the inducible antioxidative capacity. On the other hand, differences in the flux threshold of POD_Y appropriate for the linear regression could also suggest differences in the detoxification capacity in the leaves among the tree species, because the flux threshold could focus the POD to the portion of the O_3 flux that is thought to be not detoxified in the leaves. However, the rank in descending order of the flux threshold was *Q. mongolica* var. *crispula*, *F. crenata*, *Q. serrata* and *B. platyphylla* var. *japonica* (Table 4) and did not match with that of the λ (Figure 2). The flux threshold of Y is the cut-off O_3 flux at a constant value throughout the growing season, even though the detoxification capacity in the leaves changes not only owing to O_3 exposure but also owing to leaf aging. Thus, the flux threshold of Y might not be biologically relevant. To make quantification of O_3 damage on photosynthetic CO_2 uptake more mechanistic and biologically relevant, therefore, further study is required to clarifying the mechanisms underlying the different response of ΣP_{n_est} to POD_0 among the species with emphasis not only on constitutive but also on inducible and phenological changes in antioxidative capacity in the leaves [14,15,44].

Although Lombardozzi et al. (2013) [39] did not observe any correlations between changes in A_{sat} and POD based on the data from the peer-reviewed literature, part of the literature could be useful for establishment of photosynthetic responses to POD, which could be easily incorporated into models of the carbon cycling. In the present study, O_3-induced reductions in net photosynthetic rate were greater under relatively high light intensities and tended to be similar above a PPFD of approximately 500 μmol m^{-2} s^{-1} (e.g., Figure S1), which was also observed in a study by Coleman et al. (1995) [41]. This result suggests that the O_3-induced reduction in A_{sat} considerably accounts for the reduction in the ΣP_{n_est}. Across the species and leaf types, we found a significant linear correlation, with a slope of 0.93, between the relative value of ΣP_{n_est} and that of ΣA_{sat} × days, which is parameter similar to seasonal mean percent reduction in A_{sat} as reported by Novak et al. (2005) [29] (Figure 3). Several data points, which were obtained from the leaves with a short cumulative period, such as the 2nd flush leaves of *Q. serrata* and *Q. mongolica* var. *crispula* and the late leaves of *B. platyphylla* var. *japonica*, were plotted slightly away from the 1:1 line. This could result from the low number of measurements taken during the accumulation period. Therefore, the A_{sat}, if measured at appropriate intervals throughout the growing season, could be used to evaluate the O_3-induced percent change in ΣP_{n_est}. Several researchers have reported such seasonal measurements of A_{sat} in the leaves of deciduous broad-leaved tree species [40,49–51]. These data sets could be used to estimate the degree of O_3-induced reduction in cumulative photosynthetic CO_2 uptake and its response to stomatal O_3 uptake, which is useful in the quantification of the negative impact of O_3 on the NPP of deciduous broad-leaved forest trees.

5. Conclusions

In the present study, the cumulative photosynthetic CO_2 uptake of four representative Japanese deciduous broad-leaved forest tree species was estimated from *A*-light curves measured periodically during the growing season. The whole-plant-level ΣP_{n_est} were highly correlated with the whole-plant dry mass increments over the two growing seasons. Because whole-plant growth is largely determined by the amount of leaf area per plant and net photosynthetic rate per leaf area, this result suggests that leaf-level ΣP_{n_est}, which was estimated from the monthly *A*-light curves and hourly PPFD, could reflect the cumulative photosynthetic CO_2 uptake of the seedlings per unit LA. The ΣA_{sat}×days calculated from periodically measured A_{sat} could be used to evaluate the O_3-induced percent change in leaf-level ΣP_{n_est}. Although the O_3-induced percent changes in leaf-level ΣP_{n_est} were well explained by POD_0 in all the tree species, species-specific responses of leaf-level ΣP_{n_est} to POD_0 were observed. In addition, the flux threshold appropriate for the linear regression of the responses of relative leaf-level ΣP_{n_est} to POD was also species-specific. Therefore, species-specific responses of cumulative photosynthetic CO_2 uptake to stomatal O_3 uptake could be used for more accurate evaluations of O_3 impact on the NPP of Japanese deciduous broad-leaved forest tree species.

Supplementary Materials: The following are available online at http://www.mdpi.com/1999-4907/10/7/556/s1: Table S1: Monthly means of air temperature, vapor pressure deficit (VPD) and photosynthetic photon flux density

(PPFD) inside the chambers during the O_3-exposure periods in 2012 and 2013, Table S2: SUM00, AOT40 and POD_0 corresponding to each A_{sat} in 2012 and 2013, Table S3: Results of the parameterization of the stomatal conductance models, Table S4: POD_0, ΣP_{n_est} and ΣA_{sat}×days in 2012 and 2013, Table S5: Actual air temperatures inside the leaf chamber for measuring gas exchange rates, Table S6: Results of fitting the light-response curve of photosynthesis with non-rectangular hyperbolic function, Table S7: Light-saturated net photosynthetic rate at photosynthetic photon flux density of 1500 μmol m^{-2} s^{-1} (A_{sat}, μmol m^{-2} s^{-1}) in 2012 and 2013, Table S8: Effects of O_3 on the whole-plant dry mass at the end of the exposure in October and November 2013, Figure S1: Typical effect of O_3 on light response curve of net photosynthesis (*A*-light curve) observed in the present study.

Author Contributions: Conceptualization, T.I. and H.M.; Methodology, T.I. and H.M.; Investigation, H.M., M.Y. and Y.K.; Resources, H.M.; Writing—Original draft preparation, M.Y. and Y.K.; Writing—Review & editing, T.I. and H.M.; Visualization, M.Y.; Supervision, T.I.; Funding acquisition, T.I.

Funding: This research was funded by the Ministry of the Environment, Japan, through the Program of the Environment Research and Technology Development Fund, grant number 5B-1105.

Acknowledgments: The authors acknowledge Takeshi Tange (The University of Tokyo) for his valuable suggestions. We also acknowledge Takayoshi Koike (Hokkaido University) and Mitsutoshi Kitao (Forestry and Forest Products Research Institute) for their valuable suggestions and technical support. The authors are greatly indebted to Isamu Nouchi (Association of International Research Initiatives for Environmental Studies) for his comprehensive guidance. The authors also acknowledge Nobutaka Nakamachi (Civil Engineering Research & Environmental Studies) for his technical support.

Conflicts of Interest: The authors declare no conflict of interest. The funders had no role in the design of the study; in the collection, analyses or interpretation of data; in the writing of the manuscript or in the decision to publish the results.

References

1. Fuhrer, J. Ozone risk for crops and pastures in present and future climates. *Naturwissenschaften* **2009**, *96*, 173–194. [CrossRef] [PubMed]
2. Matyssek, R.; Karnosky, D.F.; Wieser, G.; Percy, K.; Oksanen, E.; Grams, T.E.E.; Kubiske, M.; Hanke, D.; Pretzsch, H. Advances in understanding ozone impact on forest trees: Messages from novel phytotron and free-air fumigation studies. *Environ. Pollut.* **2010**, *158*, 1990–2006. [CrossRef] [PubMed]
3. Emberson, L.D.; Kitwiroon, N.; Beevers, S.; Büker, P.; Cinderby, S. Scorched Earth: How will changes in the strength of the vegetation sink to ozone deposition affect human health and ecosystems? *Atmos. Chem. Phys.* **2013**, *13*, 6741–6755. [CrossRef]
4. Wittig, V.E.; Ainsworth, E.A.; Naidu, S.L.; Karnosky, D.F.; Long, S.P. Quantifying the impact of current and future tropospheric ozone on tree biomass, growth, physiology and biochemistry: A quantitative meta-analysis. *Global Change Biol.* **2009**, *14*, 396–424. [CrossRef]
5. Watanabe, M.; Hoshika, Y.; Koike, T.; Izuta, T. Combined effects of ozone and other environmental factors on Japanese trees. In *Air pollution impacts on plant in East Asia*; Izuta, T., Ed.; Springer: Tokyo, Japan, 2017; pp. 101–110.
6. Ainsworth, E.A.; Yendrek, C.R.; Sitch, S.; Colling, W.J.; Emberson, L.D. The effects of tropospheric ozone on net primary productivity and implications for climate change. *Annu. Rev. Plant Biol.* **2012**, *63*, 637–661. [CrossRef] [PubMed]
7. Sitch, S.; Cox, P.M.; Collins, W.J.; Huntingford, C. Indirect radiative forcing of climate change through ozone effects on the land-carbon sink. *Nature* **2007**, *448*, 791–795. [CrossRef]
8. Myhre, G.; Shindell, D.; Bréon, F.-M.; Collin, W.; Fuglestvedt, J.; Huang, J.; Koch, D.; Lamarque, J.-F.; Lee, D.; Mendoza, B.; et al. Anthropogenic and Natural Radiative Forcing. In *Climate Change 2013: The Physical Science Basis. Contribution of Working Group I to the Fifth Assessment Report of the Intergovernmental Panel on Climate Change*; Stocker, T.F., Qin, D., Plattner, G.-K., Tignor, M., Allen, S.K., Boschung, J., Nauels, A., Xia, Y., Bex, V., Midgley, P.M., Eds.; Cambridge University Press: Cambridge, UK; New York, NY, USA, 2013; pp. 679–681.
9. Ohara, T.; Akimoto, H.; Kurokawa, J.; Horii, N.; Yamaji, K.; Yan, X.; Hayasaka, T. An Asian emission inventory of anthropogenic emission sources for the period 1980–2020. *Atomos. Chem. Phys.* **2007**, *7*, 4419–4444. [CrossRef]
10. Yamaji, K.; Ohara, T.; Uno, I.; Kurokawa, J.; Pochanart, P.; Akimoto, H. Future prediction of surface ozone over east Asia using Models-3 Community Multiscale Air Quality Modeling System and Regional Emission Inventory in Asia. *J Geophys.l Res.* **2008**, *113*, D08306. [CrossRef]

11. Wild, O.; Fiore, A.M.; Shindell, D.T.; Doherty, R.M.; Collins, W.J.; Dentener, F.J.; Schultz, M.G.; Gong, S.; MacKenzie, I.A.; Zeng, G.; et al. Modelling future changes in surface ozone: A parameterized approach. *Atmos. Chem. Phys.* **2012**, *12*, 2037–2054. [CrossRef]
12. Akimoto, H.; Mori, Y.; Sasaki, K.; Nakanishi, H.; Ohizumi, T.; Itano, Y. Analysis of monitoring data of ground-level ozone in Japan for long-term trend during 1990–2010: Causes of temporal and spatial variation. *Atmos. Environ.* **2015**, *102*, 302–310. [CrossRef]
13. Nouchi, I. Responses of whole plants to air pollutants. In *Air pollution and plant biotechnology—Prospects for phytomonitoring and phytoremediation*; Omasa, K., Saji, H., Youssefian, S., Kondo, N., Eds.; Springer: Tokyo, Japan, 2002; pp. 3–39.
14. Musselman, R.C.; Lefohn, A.S.; Massman, W.J.; Heath, R.L. A critical review and analysis of the use of exposure- and flux-based ozone indices for predicting vegetation effects. *Atmos. Environ.* **2006**, *40*, 1869–1888. [CrossRef]
15. Heath, R.L.; Lefohn, A.S.; Musselman, R.C. Temporal processes that contribute to nonlinearity in vegetation responses to ozone exposure and dose. *Atmos. Environ.* **2009**, *43*, 2919–2928. [CrossRef]
16. Pleijel, H.; Danielsson, H.; Karlsson, G.P.; Gelang, J.; Karlsson, P.E.; Selldén, G. An ozone flux-response relationship for wheat. *Environ. Pollut.* **2000**, *109*, 453–462. [CrossRef]
17. Büker, P.; Feng, Z.; Uddling, J.; Briolat, A.; Alonso, R.; Braun, S.; Elvira, S.; Gerosa, G.; Karlsson, P.E.; Le Thiec, D.; et al. New flux based dose-response relationships for ozone for European forest tree species. *Environ. Pollut.* **2015**, *206*, 163–174. [CrossRef] [PubMed]
18. CLRTAP. Mapping critical levels for vegetation. Chapter III of Manual on methodologies and criteria for modelling and mapping critical loads and levels and air pollution effects, risks and trends. 2017. UNECE Convention on Long-range Transboundary Air Pollution. Available online: www.icpmapping.org (accessed on 5 May 2019).
19. Larcher, W. The exchange of carbon dioxide and oxygen. In *Physiological Plant Ecology*, 4th ed.; Larcher, W., Ed.; Springer: Berlin/Heidelberg, Germany, 2003; pp. 91–100.
20. Jarvis, P.G. The interpretation of the variations in leaf water potential and stomatal conductance found in canopies in the field. *Philos. Trans. R. Soc. Lond. B. Biol. Sci.* **1976**, *273*, 593–610. [CrossRef]
21. Grüters, U.; Fangmeier, A.; Jäger, H.-J. Modelling stomatal responses of spring wheat (*Triticum aestivum* L. cv. Turbo) to ozone and different levels of water supply. *Environ. Pollut.* **1995**, *87*, 141–149. [CrossRef]
22. Emberson, L.D.; Wieser, G.; Ashmore, M.R. Modelling of stomatal conductance and ozone flux of Norway spruce: Comparison with field data. *Environ. Pollut.* **2000**, *109*, 393–402. [CrossRef]
23. Hoshika, Y.; Hajima, T.; Shimizu, Y.; Takigawa, M.; Omasa, K. Estimation of stomatal ozone uptake of deciduous trees in East Asia. *Ann. For. Sci.* **2011**, *68*, 607–616. [CrossRef]
24. Hoshika, Y.; Paoletti, E.; Omasa, K. Parameterization of *Zelkova serrata* stomatal conductance model to estimate stomatal ozone uptake in Japan. *Atmos. Environ.* **2012**, *55*, 271–278. [CrossRef]
25. Hoshika, Y.; Watanabe, M.; Inada, N.; Koike, T. Modeling of stomatal conductance for estimating ozone uptake of *Fagus crenata* under experimentally enhanced free-air ozone exposure. *Water Air Soil Pollut.* **2012**, *223*, 3893–3901. [CrossRef]
26. Azuchi, F.; Kinose, Y.; Matsumura, T.; Kanomata, T.; Uehara, Y.; Kobayashi, A.; Yamaguchi, M.; Izuta, T. Modeling stomatal conductance and ozone uptake of *Fagus crenata* grown under different nitrogen loads. *Environ. Pollut.* **2014**, *184*, 481–487. [CrossRef] [PubMed]
27. Kinose, Y.; Azuchi, F.; Uehara, Y.; Kanomata, T.; Kobayashi, A.; Yamaguchi, M.; Izuta, T. Modeling of stomatal conductance to estimate stomatal ozone uptake by *Fagus crenata*, *Quercus serrata*, *Quercus mongolica* var. *crispula* and *Betula platyphylla*. *Environ. Pollut.* **2014**, *194*, 235–245. [CrossRef] [PubMed]
28. Wittig, V.E.; Ainsworth, E.A.; Long, S.P. To what extent do current and projected increases in surface ozone affect photosynthesis and stomatal conductance of trees? A meta-analytic review of the last 3 decades of experiments. *Plant Cell Environ.* **2007**, *30*, 1150–1162. [CrossRef] [PubMed]
29. Novak, K.; Schaub, M.; Fuhrer, J.; Skelly, J.M.; Hug, C.; Landolt, W.; Bleuler, P.; Kräuchi, N. Seasonal trends in reduced leaf gas exchange and ozone-induced foliar injury in three ozone sensitive woody plant species. *Environ. Pollut.* **2005**, *136*, 33–45. [CrossRef] [PubMed]
30. Nakashizuka, T.; Iida, S. Composition, dynamics and disturbance regime of temperate deciduous forests in Monsoon Asia. *Vegetatio* **1995**, *121*, 23–30. [CrossRef]
31. Koike, T. Leaf structure and photosynthetic performance as related to the forest succession of deciduous broad-leaved trees. *Plant Species Biol.* **1988**, *3*, 77–87. [CrossRef]

32. Kohno, Y.; Matsumura, H.; Ishii, T.; Izuta, T. Establishing critical levels of air pollutants for protecting East Asian vegetation—A challenge. In *Plant Responses to Air Pollution and Global Change*; Omasa, K., Nouchi, I., De Kok, L.J., Eds.; Springer: Tokyo, Japan, 2005; pp. 243–250.
33. Yamaguchi, M.; Watanabe, M.; Matsumura, H.; Kohno, Y.; Izuta, T. Experimental studies on the effects of ozone on growth and photosynthetic activity of Japanese forest tree species. *Asian J. Atmos. Environ.* **2011**, *5*, 65–78. [CrossRef]
34. Brown, K.A.; Roberts, T.M. Effects of ozone on foliar leaching in Norway spruce (*Picea abies* L. Karst): Confounding factors due to NOx production during ozone generation. *Environ. Pollut.* **1988**, *55*, 55–73. [CrossRef]
35. Laisk, A.; Kull, O.; Moldau, H. Ozone concentration in leaf intercellular air spaces is close to zero. *Plant Physiol.* **1989**, *90*, 1163–1167. [CrossRef] [PubMed]
36. Massman, W.J. A review of the molecular diffusivities of H_2O, CO_2, CH_4, CO, O_3, SO_2, NH_3, N_2O, NO and NO_2 in air, O_2 and N_2 near STP. *Atmos. Environ.* **1998**, *32*, 1111–1127. [CrossRef]
37. Webb, R.A. Use of the boundary line in the analysis of biological data. *J. Hortic. Sci.* **1972**, *47*, 309–319. [CrossRef]
38. Rawlings, J.O.; Lesser, V.M.; Dassel, K. Statistical approaches to assessing crop losses. In *Assessment of Crop Loss from Air Pollutants*; Heck, W.W., Taylor, O.C., Tingey, D.T., Eds.; Elsevier Science Publishers: Essex, UK, 1988; pp. 389–416.
39. Lombardozzi, D.; Sparks, J.P.; Bonan, G. Integrating O_3 influences on terrestrial processes: Photosynthetic and stomatal response data available for regional and global modeling. *Biogeosciences* **2013**, *10*, 6815–6831. [CrossRef]
40. Yonekura, T.; Honda, Y.; Oksanen, E.; Yoshidome, M.; Watanabe, M.; Funada, R.; Koike, T.; Izuta, T. The influences of ozone and soil water stress, singly and in combination, on leaf gas exchange rates, leaf ultrastructural characteristics and annual ring width of *Fagus crenata* seedlings. *J. Jpn. Soc. Atmos. Environ.* **2001**, *36*, 333–351.
41. Coleman, M.D.; Isebrands, J.G.; Dickson, R.E.; Karnosky, D.F. Photosynthetic productivity of aspen clones varying in sensitivity to tropospheric ozone. *Tree Physiol.* **1995**, *15*, 585–592. [CrossRef] [PubMed]
42. Hoshika, Y.; Carriero, G.; Feng, Z.; Zhang, Y.; Paoletti, E. Determinants of stomatal sluggishness in ozone-exposed deciduous tree species. *Sci. Tot. Environ.* **2014**, *481*, 453–458. [CrossRef]
43. Zhang, W.; Feng, Z.; Wang, X.; Niu, J. Responses of native broadleaved woody species to elevated ozone in subtropical China. *Environ. Pollut.* **2012**, *163*, 149–157. [CrossRef] [PubMed]
44. Matyssek, R.; Sandermann, H.; Wieser, G.; Booker, F.; Cieslik, S.; Musselman, R.; Ernst, D. The challenge of making ozone risk assessment for forest trees more mechanistic. *Environ. Pollut.* **2008**, *156*, 567–582. [CrossRef]
45. Dizengremel, P.; Thiec, D.L.; Hasenfratz-Sauder, M.-P.; Vaultier, M.-N.; Bagard, M.; Jolivet, Y. Metabolic-dependent changes in plant cell redox power after ozone exposure. *Plant Biol.* **2009**, *11*, 35–42. [CrossRef]
46. Matyssek, R.; Bytnerowicz, A.; Karlsson, P.-E.; Paoletti, E.; Sanz, M.; Schaub, M.; Wieser, G. Promoting the O_3 flux concept for European forest trees. *Environ. Pollut.* **2007**, *146*, 587–607. [CrossRef]
47. Long, S.P.; Naidu, S.L. Effects of oxidants at the biochemical, cell and physiological levels, with particular reference to ozone. In *Air Pollution and Plant Life*, 2nd ed.; Bell, J.N.B., Treshow, M., Eds.; John Wiley & Sons Ltd.: Chichester, UK, 2002; pp. 69–88.
48. Wieser, G.; Matyssek, R. Linking ozone uptake and defense towards a mechanistic risk assessment for forest trees. *New Phytol* **2007**, *174*, 7–9. [CrossRef]
49. Bortier, K.; Ceulemans, R.; De Temmerman, L. Effects of ozone exposure on growth and photosynthesis of beach seedlings (*Fagus sylvatica*). *New Phytol* **2000**, *146*, 271–280. [CrossRef]
50. Oksanen, E. Responses of selected birch (*Betula pendula* Roth) clones to ozone change over time. *Plant Cell Environ.* **2003**, *26*, 875–886. [CrossRef] [PubMed]
51. Uddling, J.; Karlsson, P.E.; Glorvigen, A.; Sellden, G. Ozone impairs autumnal resorption of nitrogen from birch (*Betula pendula*) leaves, causing an increase in whole-tree nitrogen loss through litter fall. *Tree Physiol.* **2006**, *26*, 113–120. [CrossRef] [PubMed]